

Research article

DEVELOPMENTAL EXPRESSION OF P₅ ATPASE mRNA IN THE MOUSE

LISA S. WEINGARTEN¹, HARDI DAVE², HONGYAN LI²
 and DOROTA A. CRAWFORD^{1,2,3*}

¹Department of Biology, York University, Faculty of Science and Engineering,
 4700 Keele Street, Bethune College, Toronto, Ontario M3J-1P3, Canada,

²School of Kinesiology and Health Science, Faculty of Health, York University,
 Toronto, Canada, ³Neuroscience Graduate Diploma Program, Faculty of Health,
 York University, Toronto, Canada

Abstract: P₅ ATPases (ATP13A1 through ATP13A5) are found in all eukaryotes. They are currently poorly characterized and have unknown substrate specificity. Recent evidence has linked two P₅ ATPases to diseases of the nervous system, suggesting possible importance of these proteins within the nervous system. In this study we determined the relative expression of mouse P₅ ATPases in development using quantitative real time PCR. We have shown that *ATP13A1* and *ATP13A2* were both expressed similarly during development, with the highest expression levels at the peak of neurogenesis. *ATP13A3* was expressed highly during organogenesis with one of its isoforms playing a more predominant role during the period of neuronal development. *ATP13A5* was expressed most highly in the adult mouse brain. We also assessed the expression of these genes in various regions of the adult mouse brain. *ATP13A1* to *ATP13A4* were expressed differentially in the cerebral cortex, hippocampus, brainstem and cerebellum while levels of *ATP13A5* were fairly constant between these brain regions. Moreover, we demonstrated expression of the ATP13A4

* Author for correspondence. e-mail : dake@yorku.ca, phone: 416-736-2100 ext. 23324, fax: 416-736-5774

Abbreviations used: ASD – autism spectrum disorders; B2m – beta-2-microglobulin; DAB – 3,3'-diaminobenzidine; DTT – dithiothreitol; Gapdh – glyceraldehyde 3-phosphate dehydrogenase; Gusb – beta-glucuronidase; HPRT – hypoxanthine phosphoribosyl transferase; NGS – normal goat serum; PBS – phosphate buffered saline; PBS-T – phosphate buffered saline Tween 20; PCR – polymerase chain reaction; PD – Parkinson's disease; PFA – paraformaldehyde; Pgk1 – phosphoglycerate kinase 1; qPCR – quantitative polymerase chain reaction; Tfrc – transferring receptor

protein in the corresponding brain regions using immunohistochemistry. In summary, this study furthers our knowledge of P₅-type ATPases and their potentially important role in the nervous system.

Key words: P₅-type ATPases, mRNA expression, Neurogenesis, Parkinson's disease, Autism spectrum disorders, Real-time PCR, Immunohistochemistry

INTRODUCTION

The P-type superfamily of ATPases comprises a family containing more than 50 different transmembrane proteins which transport inorganic cations or other substrates, such as phospholipids, across membranes within the cell [1-5]. P-type ATPases are found within both prokaryotes and eukaryotes and have been classified into five subfamilies based on their substrate specificity. P₁ ATPases include the IA bacterial ion pumps which transport ions such as K⁺, and the IB pumps, found in bacteria, plants, and animals, which transport transition metals such as Cu²⁺, Cd²⁺, and Zn²⁺. The P₂ family is the most diverse of the five families and includes Ca²⁺, Na⁺/K⁺, H⁺/K⁺ ATPases found in bacteria, animals and some fungi. P₃ ATPases include H⁺ and Mg²⁺ ATPases in bacteria, plants and lower eukaryotes. P₄ ATPases are found exclusively in eukaryotes and transport aminophospholipids across membranes. P₅ ATPases are also found only in eukaryotes and their substrate specificity and biological role are not clearly determined [2, 3].

The P₅ family of ATPases is expressed only in eukaryotes and was first identified in yeasts. Two P₅ ATPases have been identified in yeasts, Cod1p/Spf1p and Yor291wp. Cod1p is localized to the endoplasmic reticulum and has been shown to play a role in calcium homeostasis although it does not exhibit kinetics typical of Ca²⁺ pumps [6, 7]. Interestingly, our previous study illustrated that *ATP13A4*, localized to the endoplasmic reticulum, may also play a role in regulating intracellular calcium levels in mammalian cell culture [8]. It has been suggested that P₅ ATPases may also transport nonmetallic substrates or couple with other proteins which transport Ca²⁺ or regulate Ca²⁺ levels. While the substrate specificity of these ATPases is still being investigated, they have been reported to play important roles in many cellular processes, including glycosylation [9], protein secretion and trafficking [10, 11], and the unfolded protein response [9, 10, 12, 13].

Two subfamilies of P₅ ATPases (P_{5A} and P_{5B}) are found in eukaryotes [2]. The negatively charged amino acids (D or E) in the 5A ion-binding site are replaced with hydrophobic amino acids (A or V) in the 5B ion-binding site, likely indicating different ion specificities for P_{5A} and P_{5B} ATPases [14]. In humans, five P₅ ATPases have been identified. The P_{5A} subfamily contains *ATP13A1*, and the P_{5B} subfamily contains *ATP13A2*, *ATP13A3*, *ATP13A4*, and *ATP13A5* [15]. Homologues of these five proteins exist in the mouse [16]. Based on phylogenetic analysis, it has been hypothesized that *ATP13A1* is derived from

the yeast orthologue Cod1p and the P_{5B} ATPases (*ATP13A2-A5*) are derived from the yeast orthologue Yor291wp, with *ATP13A4* and *ATP13A5* having the greatest degree of homology and therefore likely the closest evolutionary relationship [15, 16]. The mRNA tissue distribution of P₅ ATPases in the mouse illustrates that *ATP13A1-A3* are expressed at significant levels in a variety of organs, including the brain, colon, kidney, liver, intestine, stomach and skeletal muscle; however, *ATP13A4* and *ATP13A5* are primarily expressed in the brain and stomach [16]. It was also observed that alternative splicing results in the expression of two *ATP13A3* mRNA transcript variants which produce different isoforms of the *ATP13A3* protein. Transcript variant 1 contains one additional exon (exon 30) at the 5' end of the transcript compared with transcript variant 2 and produces a protein with an additional 30 amino acids at the C-terminal end. These two mRNA variants are differentially expressed in different body tissues, with transcript variant 1 preferentially expressed in the brain, heart, and lung, and transcript variant 2 preferentially expressed in the kidney, small intestine, and testis [16].

Recent studies have shown that mutations within two P_{5B} ATPase genes, *ATP13A2* and *ATP13A4*, contribute to the development of early-onset Parkinson's disease (PD) and autism, respectively [15, 17-19]. Moreover, Ramirez *et al.* identified homozygous missense and nonsense mutations in *ATP13A2* (*PARK9*) as the cause of Kufor-Rakeb disease, a recessive, juvenile onset atypical Parkinsonism accompanied by dementia, and reported elevated levels of *ATP13A2* mRNA in PD patients [17]. Sequence variations in *ATP13A2* have been linked to early onset PD in populations in Taiwan and Singapore [19] and homozygous missense mutations in this gene have been shown to contribute to the development of PD [18]. No correlation has been found between *ATP13A2* and late onset Parkinson's disease [20]. We have previously identified an inherited chromosomal inversion which disrupted the *ATP13A4* gene in a patient with expressive and receptive language delay [15]. We also found a sequence variant within *ATP13A4*, which resulted in the substitution of aspartic acid for a glutamic acid (E646D) in individuals with autism spectrum disorders (ASD) [15]. These recent discoveries suggest an important role for the P₅ ATPases in the nervous system. Defects in these genes may have differing effects on the development of the nervous system depending on the spatial and temporal expression characteristics of the genes involved.

In this study, we examined whether gene expression of P₅ ATPases is developmentally regulated. We assessed the expression of mRNAs in the mouse at days 7, 11, 15, and 17 of embryogenesis using quantitative real-time PCR. In order to elucidate possible functional roles of P₅ ATPases in the nervous system, we also assessed the mRNA expression levels in selected regions of the adult mouse brain, including cerebral cortex, frontal cortex, hippocampus, brainstem and cerebellum. Moreover, we also confirmed the expression of the *ATP13A4* protein in these brain regions with immunohistochemistry. Our study shows that the expression of the P₅ ATPase genes appears to be developmentally regulated

and they may play an important role in early development. We also illustrate that the expression of these ATPases varies throughout the mature nervous system and each member of this subfamily shows a unique distribution throughout the major regions of the adult brain.

MATERIALS AND METHODS

cDNA synthesis by MMuLV reverse transcriptase

Total RNA from mouse embryos at 7, 11, 15, and 17 days of gestation (E7, E11, E15, E17), adult mouse brain, and specific regions of adult mouse brain (cerebellum, cerebral cortex, frontal cortex, hippocampus, and brainstem) derived from BALB/c mice was obtained from Clontech Laboratories. The RNA was pooled from 200-800 male and/or female mice at appropriate ages. To prepare cDNA from each of these samples, 2 µg of an RNA sample was incubated with 50 units of MMuLV reverse transcriptase (Stratagene) in 1x MMuLV reverse transcriptase reaction buffer (Stratagene) containing 0.01 M DTT (dithiothreitol), 0.4 mM dNTPs, and 0.5 µg Oligo(dT)₁₂₋₁₈ (New England Biolabs) and DEPC treated (0.1%) distilled water to a final reaction volume of 50 µl. The reaction was incubated at 37°C for 1 hour and the resulting cDNAs were used for quantitative real-time PCR analysis or stored at +4°C.

Quantitative real time PCR

The expression of the various P₅-type ATPases in each of the RNA samples was determined using the 7500 Fast Real Time PCR system (Applied Biosystems) with SYBR Advantage qPCR Premix (Clontech Laboratories). The Applied Biosystems 7500 Fast version 1.3.1 software was used to calculate the threshold cycle (C_t) and determine the relative quantity of the different samples. Analysis was performed using the $\Delta\Delta C_t$ method, where relative quantity (RQ) = $2^{-\Delta\Delta C_t}$ and $\Delta\Delta C_t = \Delta C_{t, \text{sample}} - \Delta C_{t, \text{reference}}$. $\Delta C_{t, \text{sample}}$ is the difference in threshold cycle between any developmental stage or brain region and the endogenous reference gene hypoxanthine phosphoribosyl transferase (*HPRT*) [21] and $\Delta C_{t, \text{reference}}$ is the difference in threshold cycle between the reference sample/calibrator (adult brain or cerebral cortex for the developmental expression or adult brain expression profiles, respectively) and the endogenous control (*HPRT*). Santos and Duarte found *HPRT* to be the most reliable reference gene for real-time PCR [21]. *HPRT* expression reflects the average expression of multiple common reference genes, making it the best choice when using only a single normalization gene [22]. *HPRT* has also been shown to be expressed at constant levels compared to other reference genes [21, 23-25]. To determine the stability of *HPRT* in all developmental stages used, its expression was validated against additional commonly used reference genes, including *B2m* (beta-2-microglobulin), *Gapdh* (glyceraldehyde 3-phosphate dehydrogenase), *Gusb* (beta-glucuronidase), *Tfrc* (transferrin receptor), and *Pgk1* (phosphoglycerate kinase 1) [21, 26]. The Ct value of the six genes was analyzed for validation of

expression value (M) across development using the geNorm program [27]. *HPRT*, *B2m* and *Gusb* ranked as the most stable genes. When compared to the *B2m* and *Gusb* expression, *HPRT* showed stable expression across development. To determine the relative proportions of the two transcript variants of *ATP13A3*, the ratio of the relative quantity of *ATP13A3* transcript variant 1 to the relative quantity of total *ATP13A3* was determined ($RQ\ ATP13A3_{\text{variant 1}} / RQ\ ATP13A3_{\text{total}}$). Primers were designed using the Primer Express 3.0 for Real Time PCR software (Applied Biosystems), at the exon-exon junctions within the target genes. The sequences of the primers used and the resulting amplicon lengths are listed in Tab. 1. One set of primers was designed for each of *ATP13A1*, *ATP13A2*, *ATP13A4*, *ATP13A5*, and the endogenous reference *HPRT*. Two sets of primers were designed for *ATP13A3*: one set to amplify both transcript variants 1 and 2 (*ATP13A3-F* and *-R*) while the other set was specific for transcript variant 1 (*ATP13A3-variant1-F* and *-R*), which does not contain exon 30. 2 μg of total RNA was converted to cDNA as described above. The cDNA was incubated with 1 \times SYBR Advantage qPCR Premix, 1 \times ROX LMP passive reference dye (Clontech laboratories), and 1 μM of each primer in 20 μl reaction. The amplification proceeded with an initial denaturation at 95°C for 20s, followed by 40 cycles of denaturation at 95°C for 3s and annealing/elongation at 60°C for 30s. All runs were performed in triplicate and the relative quantity of each gene was determined in three independent experiments. The same source of RNA was used for each independent experiment for the expression in the embryonic stages and the adult brain.

Tab. 1. Forward (F) and reverse (R) primer sequences for quantitative real-time PCR.

Primer name	Sequence (5' \rightarrow 3')	Amplicon length (bp)
ATP13A1-F	ACC CTG CAC TCT ATG TTT TCT CAG T	71
ATP13A1-R	CCT TCC CGA GAG ATC TCA GTG T	71
ATP13A2-F	CGC CGA AAC ACT CGT TAT AGA A	68
ATP13A2-R	CCT GAA CCG TGA AGA GCT GTC T	68
ATP13A3-F	TGA AGC TTC CGT GGC ATC TC	81
ATP13A3-R	GCA CGA CCT TCC CTG ATA AGG	81
ATP13A3-variant1-F	CTA TCA CGG TGG AGA GCT TCT TC	83
ATP13A3-variant1-R	GAA ACG ACA CTC TCC TTG TTT GTC T	83
ATP13A4-F	GGC AGC CCA CCT ATA CAA ACT ATA TAT	72
ATP13A4-R	GAA TGA AAA GAC ATA CGC CCA TCT	72
ATP13A5-F	GAG TGA GGC CCG CAT CAG	67
ATP13A5-R	AGC AAC AGT GAT GGC AGT TTG A	67
HPRT-F	TCC ATT CCT ATG ACT GTA GAT TTT ATC AG	75
HPRT-R	AAC TTT TAT GTC CCC CGT TGA CT	75

Immunohistochemistry

The experiments were performed on C57Bl6/J adult (8 weeks) mice. All animal procedures were performed strictly in accordance with the York University Animal Care Committee guidelines. Mice were anesthetized and perfused transcardially, first with phosphate buffered saline (PBS) and then with 4% paraformaldehyde (PFA) in 0.1 M PBS (pH 7.4). The brains were removed, post-fixed in fresh PFA for 3 days at 4°C, and cryoprotected in 30% sucrose. The brains were then embedded in paraffin and cut into 4 µm thick sections (Toronto Centre for Phenogenomics). Affinity purified rabbit anti-mouse ATP13A4 antibody was developed by Affinity Bioreagents for the epitope INRAIRKPKDLKVR, which is conserved among species and located between the first two transmembrane domains (amino acids 117-130) [8]. Anti-ATP13A4 was diluted to 4 µg/ml in PBS containing 0.3% Triton-X (PBS-T) and 2% normal goat serum (NGS), and was applied to deparaffinized brain section for 24 hours at 4°C. A control experiment was conducted, omitting the primary antibodies. The antibody specificity and cross-reactivity were tested by pre-incubation of the primary antibody with the immunizing peptide (100 µg/ml) for 16 hr at 4°C. After the primary antibody treatment, sections were rinsed in PBS-T, then incubated with biotinylated rabbit anti-sheep secondary antibody (Vector Laboratories) containing 2% NGS for 1 hour followed by an avidin-biotinylated horseradish peroxidase complex (ABC Elite, Vector Laboratories). The immunoreactivity was assessed using 3,3'-diaminobenzidine (DAB) plus nickel ammonium sulfite as a chromogen. After staining, tissue sections were preserved in *Permount* mounting medium (Fisher Scientific) and images were captured and analyzed using a Nikon Eclipse 80i light microscope.

Statistical analysis

Student's two-tailed, unpaired T tests were performed on all relative quantity data to determine the statistical significance of the differences between the means. Values were deemed statistically significant at $p \leq 0.05$. All values are presented as the mean relative quantity \pm SEM.

RESULTS

Developmental expression of P₅-type ATPases

Quantitative real time PCR was performed to determine the expression profile of the P₅ ATPases in the mouse embryo to evaluate the importance of these proteins in development. The mRNA expression was assessed in various mouse developmental stages (embryonic days 7, 11, 15 and 17) and the entire adult brain. The expression of the P₅ ATPases in the various tissues was normalized to the expression of the *HPRT* gene. Our results show that *ATP13A1* and *ATP13A2* have a very similar expression patterns throughout the stages of development (Fig. 1A and 1B). Both genes showed a significant increase of expression as development progressed, with the highest expression at the peak of neurogenesis

(E15) ($p < 0.001$), which normally occurs from days 12-17 of mouse embryonic development [28]. After E15, the level of gene expression decreased rapidly, with E17 containing levels of mRNA lower than that observed at any other stage of development (Fig. 1A and 1B). The relative quantities of *ATP13A1* transcripts at E7, E11, E15, and E17 were 1.9 ± 0.5 , 5.7 ± 0.7 , 17.8 ± 1.5 , and 0.7 ± 0.2 respectively (Fig. 1A). Similarly, the relative quantities of *ATP13A2* transcripts were 1.9 ± 0.2 , 5.0 ± 1.4 , 19.6 ± 3.1 , and 0.7 ± 0.3 at E7, E11, E15, and E17 respectively (Fig. 1B). These results indicate that both *ATP13A1* and *ATP13A2* may play a role during early neuronal development.

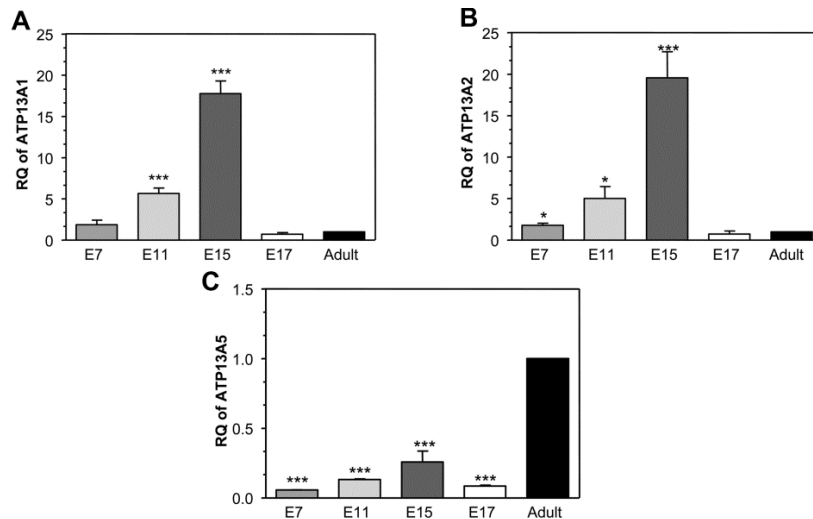


Fig. 1. Developmental expression of *ATP13A1*, *ATP13A2*, and *ATP13A5* in the mouse. Relative quantity (RQ) was calculated in embryonic day 7, 11, 15, 17 mouse tissues (E7, E11, E15, and E17 respectively) using the $\Delta\Delta C_t$ method with the adult brain taken as the calibrator (reference sample) and normalized to *HPRT*. The RQ values for E7, E11, E15, E17 were: A – 1.9 ± 0.5 , 5.7 ± 0.7 , 17.8 ± 1.5 , and 0.7 ± 0.2 for *ATP13A1*, B – 1.9 ± 0.2 , 5.0 ± 1.4 , 19.6 ± 3.1 , and 0.7 ± 0.3 for *ATP13A2*, C – 0.055 ± 0.002 , 0.131 ± 0.004 , 0.26 ± 0.08 , and 0.085 ± 0.006 for *ATP13A5*. * $p < 0.05$ *** $p < 0.001$. Values are plotted as the mean of three independent experiments \pm SEM and each sample was run in triplicate.

The relative quantity of *ATP13A5*, unlike the previous two genes, was significantly lower in the early embryonic stages but high in the adult mouse brain ($p < 0.001$). E7, E11, E15 and E17 showed relative quantity levels of 0.055 ± 0.002 , 0.131 ± 0.004 , 0.26 ± 0.08 , and 0.085 ± 0.006 (Fig. 1C). During embryonic development, the expression of *ATP13A5* showed a slight increase, peaking in E15 and returning to low levels by E17. The developmental expression profile of this gene suggests that *ATP13A5* may play a more prominent role in adult brain function. We previously determined that *ATP13A4* was expressed at low levels in E7 and E11 and increased between E11 and E15, with E17 having the highest expression of the gene, indicating that *ATP13A4* likely plays a role during later stages of neurogenesis [8].

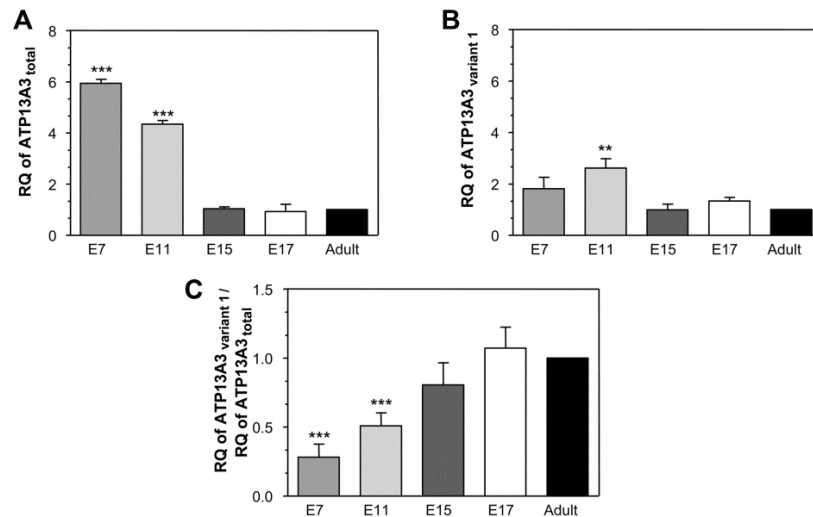


Fig. 2. Developmental expression of *ATP13A3* in the mouse. A – Total *ATP13A3* expression determined using primers amplifying both variants of *ATP13A3*. RQ values for E7, E11, E15 and E17 was 5.9 ± 0.2 , 4.3 ± 0.1 , 1.04 ± 0.07 , and 0.9 ± 0.3 respectively. B – Expression of *ATP13A3* variant 1. RQ values for E7, E11, E15, and E17 relative to the adult brain was 1.9 ± 0.4 , 2.6 ± 0.4 , 1.0 ± 0.2 , and 1.3 ± 0.1 respectively. C – Ratio of the relative quantity of *ATP13A3* variant 1 to total *ATP13A3* was 0.28 ± 0.09 , 0.51 ± 0.09 , 0.81 ± 0.2 , and 1.07 ± 0.2 for E7, E11, E15, and E17. $**p < 0.01$ $***p < 0.001$. Values are plotted as the mean of three independent experiments \pm SEM and each sample was run in triplicate.

The expression of *ATP13A3* was studied on three levels: i) the total expression of *ATP13A3* transcripts (variant 1 and 2), ii) the expression of transcript variant 1 of *ATP13A3*, and iii) the ratio of expression of transcript variant 1 to the total expression of *ATP13A3*. Total *ATP13A3* expression decreased during embryonic development, with the highest relative quantity value observed in E7 ($p < 0.001$) and E11 ($p < 0.001$) (Fig. 2A). The relative quantity values were 5.9 ± 0.2 , 4.3 ± 0.1 , 1.04 ± 0.07 , and 0.9 ± 0.3 for E7, E11, E15 and E17, respectively. Our results also show that the expression of *ATP13A3* transcript variant 1 was most highly expressed in 11 day embryos ($p < 0.01$), and expression during other developmental stages was not significantly different from the adult brain (Fig. 2B). Relative quantity values were 1.9 ± 0.4 , 2.6 ± 0.4 , 1.0 ± 0.2 , and 1.3 ± 0.1 for E7, 11, 15, and 17, respectively. The higher expression during early developmental stages likely indicates that *ATP13A3* plays a more important role during early organogenesis. Finally, the ratio of variant 1 expression to total *ATP13A3* expression was observed to increase during development, with lower expression in E7 and E11 ($p < 0.001$) (Fig. 2C). This trend indicates that a larger proportion of *ATP13A3* is expressed as variant 1 as development progresses. Relative quantity values were 0.28 ± 0.09 , 0.51 ± 0.09 , 0.8 ± 0.2 , and 1.1 ± 0.2 for E7, E11, E15, and E17, respectively. These findings demonstrate that *ATP13A3* may

play a role in mouse development and the different transcriptional variants of this gene are differentially expressed throughout development.

Spatial expression of P₅ ATPases in the adult mouse brain

The *ATP13A1-5* mRNA expression was also assessed within the selected regions of the adult brain (cerebral cortex, frontal cortex, hippocampus, brainstem, and cerebellum) using quantitative real time PCR. The expression of the P₅ ATPases in each brain region was normalized to the expression of the *HPRT* gene and was compared to the expression within the cerebral cortex. Our data show that *ATP13A1* was differentially expressed throughout the adult mouse brain, with the highest expression in the cerebellum ($p < 0.001$) and the lowest expression in the hippocampus ($p < 0.01$) (Fig. 3A). Interestingly, the expression in the frontal cortex was 1.6-fold greater than that in the total cerebral cortex ($p < 0.001$). The relative quantity values were 1.56 ± 0.09 , 0.78 ± 0.05 , 1.14 ± 0.08 , and 2.8 ± 0.2 for the frontal cortex, hippocampus, brainstem and cerebellum, respectively. *ATP13A2* was expressed most highly in the frontal cortex, followed by the brainstem and cerebellum. Expression in these three brain regions was

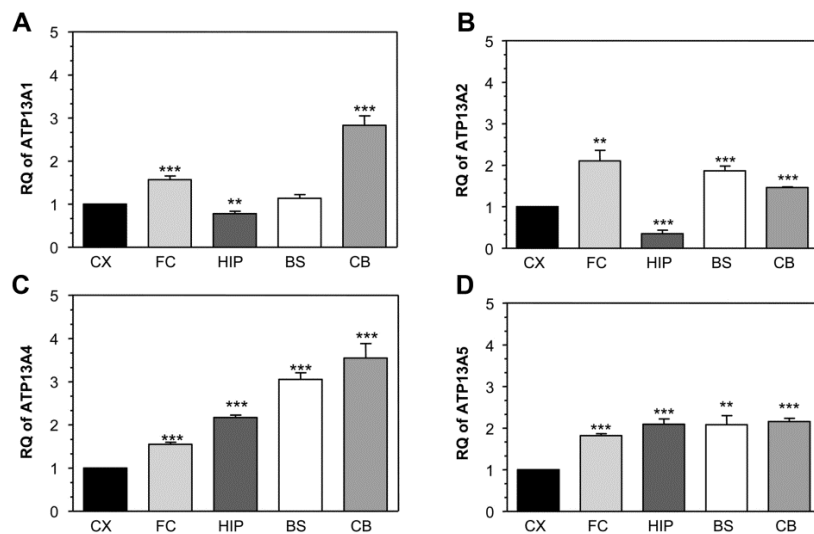


Fig. 3. *ATP13A1*, *ATP13A2*, *ATP13A4*, and *ATP13A5* expression throughout the adult mouse brain. mRNA expression was determined using quantitative real time PCR in the adult mouse brain cerebral cortex (CX), frontal cortex (FC), hippocampus (HIP), brainstem (BS) and cerebellum (CB). Relative quantity was calculated using the $\Delta\Delta C_t$ method with the cerebral cortex taken as the calibrator and normalized to *HPRT*. The RQ values in the frontal cortex, hippocampus, brainstem and cerebellum relative to the cerebral cortex (RQ=1) were: A – 1.56 ± 0.09 , 0.78 ± 0.05 , 1.14 ± 0.08 , and 2.8 ± 0.2 for *ATP13A1*, B – 2.1 ± 0.3 , 0.34 ± 0.08 , 1.9 ± 0.1 , and 1.46 ± 0.01 for *ATP13A2*, C – 1.55 ± 0.05 , 2.17 ± 0.05 , 3.0 ± 0.2 , and 3.5 ± 0.3 for *ATP13A4*, and D – 1.82 ± 0.04 , 2.1 ± 0.1 , 2.1 ± 0.2 , and 2.15 ± 0.08 for *ATP13A5*. ** $p < 0.01$ *** $p < 0.001$. Values are plotted as the mean of three independent experiments \pm SEM and each sample was run in triplicate.

statistically higher than that in the cerebral cortex ($p < 0.01$). As with *ATP13A1*, expression of *ATP13A2* was lowest in the hippocampus. The relative quantity values of the *ATP13A2* transcript compared to the cerebral cortex were 2.1 ± 0.3 , 0.34 ± 0.08 , 1.9 ± 0.1 , and 1.46 ± 0.01 for the frontal cortex, hippocampus, brainstem, and cerebellum respectively (Fig. 3B). *ATP13A4* expression was varied throughout all regions of the adult mouse brain, with the cerebellum having the highest relative expression ($p < 0.001$), followed by the brainstem ($p < 0.001$) and hippocampus ($p < 0.001$) (Fig. 3C). The *ATP13A4* mRNA transcript was also differentially expressed within the cerebral cortex, with the frontal cortex having a 1.5-fold higher expression compared to the total cerebral cortex ($p < 0.001$). Relative quantity levels compared to the cerebral cortex were 1.55 ± 0.05 , 2.17 ± 0.05 , 3.0 ± 0.2 , and 3.5 ± 0.3 in the frontal cortex, hippocampus, brainstem and cerebellum, respectively. Finally, the expression of *ATP13A5* was fairly constant throughout most of the brain regions. The relative quantity values for the frontal cortex, hippocampus, brainstem and cerebellum were 1.82 ± 0.04 , 2.1 ± 0.1 , 2.1 ± 0.2 , and 2.15 ± 0.08 respectively, relative to the cerebral cortex (Fig. 3D). These four regions showed significantly higher *ATP13A5* expression than the cerebral cortex ($p < 0.01$). These results demonstrate ubiquitous expression of the ATP13A5 protein within many regions of the adult brain.

The expression of *ATP13A3* was assayed throughout the adult brain as the total *ATP13A3* expression, the expression of only transcript variant 1 of this gene, and the ratio of the expression of variant 1 to the total *ATP13A3* expression. As seen in Fig. 4A, total *ATP13A3* was expressed to the greatest extent in the hippocampus ($p < 0.001$) followed by the cerebellum ($p < 0.001$). Expression in the frontal cortex was 1.8-fold higher than that in the entire cerebral cortex ($p < 0.001$). The expression pattern of *ATP13A3* variant 1 was very similar to that of the total *ATP13A3*. Relative quantity values in the cerebral cortex, frontal cortex, hippocampus, brainstem and cerebellum were 1.0, 1.80 ± 0.06 , 2.5 ± 0.2 , 1.14 ± 0.08 , and 2.3 ± 0.1 , respectively for total *ATP13A3*, and 1.0, 1.79 ± 0.06 , 1.99 ± 0.09 , 1.1 ± 0.1 , and 1.84 ± 0.07 respectively for variant 1 (Fig. 4B). The ratio of transcript variant 1 to total *ATP13A3* was fairly constant throughout the various brain regions, with no significant difference between the ratio values of the cerebral cortex, frontal cortex and brainstem (Fig. 4C). The ratios calculated for the hippocampus and cerebellum were only 20% lower than the ratio for the cerebral cortex, although this difference was statistically significant ($p < 0.01$ for the hippocampus and $p < 0.001$ for the cerebellum). The similarity in expression between total *ATP13A3* and transcript variant 1 expression suggests that isoform 1 of the ATP13A3 protein may be more prevalent within the adult brain than isoform 2. The values for the ratios were 1.00 ± 0.07 , 0.82 ± 0.06 , 0.95 ± 0.07 , and 0.82 ± 0.02 for the frontal cortex, hippocampus, brainstem, and cerebellum, respectively.

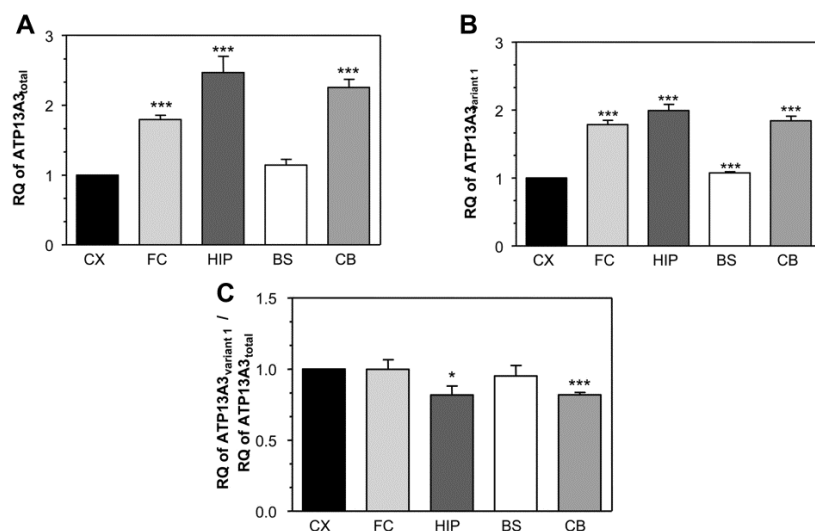


Fig. 4. *ATP13A3* expression throughout the adult mouse brain. mRNA quantification was determined in the adult mouse brain cerebral cortex (CX), frontal cortex (FC), hippocampus (HIP), brainstem (BS) and cerebellum (CB). The cerebral cortex was taken as the calibrator and data were normalized to *HPRT*. A – Total *ATP13A3* expression determined using primers that amplify both isoforms. RQ values for the frontal cortex, hippocampus, brainstem and cerebellum relative to the cerebral cortex (RQ = 1) were 1.0, 1.80 ± 0.06 , 2.5 ± 0.2 , 1.14 ± 0.08 , and 2.3 ± 0.1 respectively. B – Expression of *ATP13A3* isoform 1 determined using primers specific for only isoform 1 of *ATP13A3*. RQ for the frontal cortex, hippocampus, brainstem and cerebellum were 1.79 ± 0.06 , 1.99 ± 0.09 , 1.1 ± 0.1 , and 1.84 ± 0.07 respectively, relative to the RQ of the cerebral cortex. C – Ratio of the RQ of *ATP13A3* isoform 1 to the RQ of total *ATP13A3*. Ratios were 1.00 ± 0.07 , 0.82 ± 0.06 , 0.95 ± 0.07 , and 0.82 ± 0.02 for the frontal cortex, hippocampus, brainstem and cerebellum, respectively. * $p < 0.05$ *** $p < 0.001$. Values are plotted as the mean of three independent experiments \pm SEM and each sample was run in triplicate.

Immunohistochemical analysis of the ATP13A4 expression in the mouse brain

Antibodies for most P₅ ATPases are not commercially available, making the assessment of the encoded proteins difficult. We developed an antibody against mouse ATP13A4 (see methods) and determined the expression of this protein in the adult brain using immunohistochemistry. Our results show that ATP13A4 is widely expressed in various cells of the mouse brain (Fig. 5). Its expression appears more abundant in cells of the cerebellum, brain stem, hippocampus (particularly dentate gyrus), and frontal and motor cortex (Fig. 5A-H). This coincides with the observed mRNA expression. Controls are shown in Fig. 5I and J. We also observed that the endogenous protein was localized to the perinuclear region in brain cells (Fig. 5B, C and F), which agrees with our previous study where ATP13A4 was overexpressed in transiently transfected COS-7 cells [8].

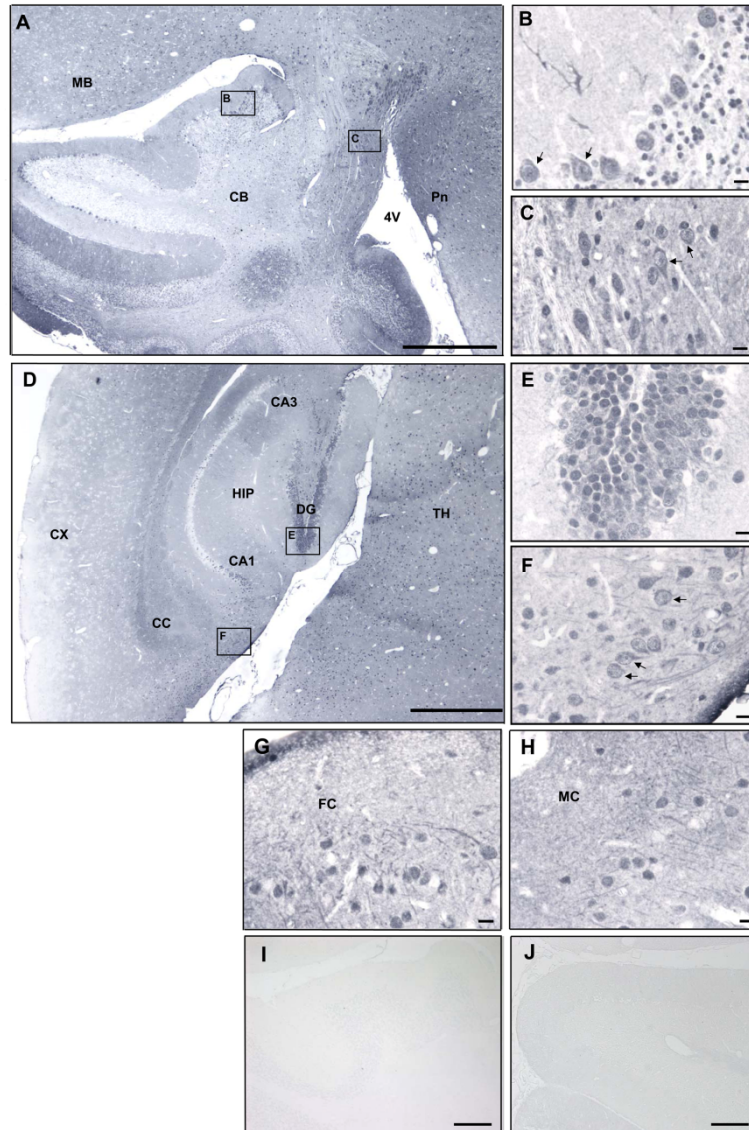


Fig. 5. Immunohistochemical detection of ATP13A4 in the mouse brain. Sagittal sections of the brain show ubiquitous expression of ATP13A4 in cells of various regions of the brain. ATP13A4 shows predominant expression in the cells of the cerebellum, midbrain, brain stem (A), hippocampus, thalamus and cortex (D), and frontal and motor cortex (G-H). Perinuclear localization of ATP13A4 is shown by arrows in the cells of the cerebellum (B-C) and hippocampus (E-F). Controls from the hippocampal region include staining without the primary antibody (I), and after pre-incubation of anti-ATP13A4 with the immunizing peptide (100 ug/ml) (J). Scale bar is 500 μm (A, D), 10 μm (B-C, E-I), and 100 μm (I, J). Abbreviations: CX – cerebral cortex, CB – cerebellum, CC – corpus callosum BS – brain stem, HIP – hippocampus, CA1 and CA3 region of the hippocampus, DG – dentate gyrus, MB – midbrain, FC – frontal cortex, MC – motor cortex, Pn – pons, TH – thalamus, 4V – 4th ventricle.

DISCUSSION

In this study we characterize the expression of the P₅ ATPases (*ATP13A1* through *ATP13A5*) during mouse development. We show that *ATP13A1* and *ATP13A2* transcript expression was the highest at the peak of neurogenesis (E15), *ATP13A3* was expressed highly during organogenesis (E7-E11), and *ATP13A5* was expressed most highly in the adult mouse brain. We previously showed that *ATP13A4* was also highly expressed at E17 during late neurogenesis [8]. The results described here provide new insights into the important role of the P₅ ATPases in embryonic development and in the nervous system.

Both *ATP13A1* and *ATP13A2* show very similar patterns of developmental expression in the mouse, with gene expression increasing until E15 and then decreasing rapidly by E17 to approximately the expression level within the adult brain. This strongly suggests that these two genes play important roles in mouse development. Moreover, since gene expression of *ATP13A1* and *ATP13A2* peaks at E15, which is in the middle of the period of neurogenesis in mice (E12 to E17) [29], it suggests that these two genes may potentially be involved specifically in the development of regions of the mouse brain. The development of the cerebral cortex, pyramidal cells and CA2 region of the hippocampus, regions of the thalamus, basal forebrain, or striatum of the brain normally peaks around day 15 of embryogenesis [29, 30].

In addition to the similarity between the developmental expression profile, *ATP13A1* and *ATP13A2* showed a similar expression profile throughout the adult mouse brain. Both showed the lowest expression within the hippocampus, high expression within the cerebellum, and greater expression within the frontal cortex compared to that of the total cortex. It is interesting to note that the expression levels of *ATP13A1* and *ATP13A2* were high at E15, the stage at which the hippocampus develops, and relatively low in the adult hippocampus. Thus, it is feasible that these two genes may play different roles at various developmental stages. The similarities observed in the developmental expression of *ATP13A1* and *ATP13A2* were unexpected due to the distant relationship predicted between these genes. *ATP13A1* is a P_{5A} ATPase while *ATP13A2* is a P_{5B} ATPase, and due to differences in the amino acid sequences of the ion binding sites of these two subclasses, they likely have different substrate specificities and different function [2, 14]. *ATP13A2/PARK9* has been recently implicated in the neurodegenerative disorders of Kufor-Rakeb disease and Parkinson's disease [17-19]. Ramirez *et al.* have shown that *ATP13A2* expression was greatest in the ventral midbrain (containing the substantia nigra) [17]. In mice, dopaminergic neurons of the substantia nigra develop prior to E15, with midbrain dopaminergic neurons generated at E11–E13 and migrating to their final positions by around E16 [31-33]. In this study we have shown that the expression of *ATP13A2* increases between E11 and E15, indicating a possibility that this protein may be involved in the development of the substantia nigra and its defect may contribute to the development of PD.

ATP13A3 mRNA is expressed as two transcript variants which differ by the inclusion of a single exon at the 5' end of the transcript [16]. In the current study, *ATP13A3* expression was assayed during development and in the adult mouse brain as total *ATP13A3*, *ATP13A3* transcript variant 1, and the ratio of transcript variant 1 to total *ATP13A3* expression. During development, total *ATP13A3* expression was greatest at E7 and decreased as development progressed, dropping to low levels at E15, E17, and in the adult mouse brain. The high levels of this transcript during early stages of mouse development, prior to the window of neurogenesis, suggests that *ATP13A3* may be involved in early organogenesis, such as the development of the digestive system, respiratory system, circulatory system, urinary system and immune system, all of which occur primarily between E7 and E11 [28]. This agrees with the previously demonstrated expression of *ATP13A3* throughout various tissues of the adult mouse, which showed very low *ATP13A3* expression in the brain and the highest levels of *ATP13A3* expression in the kidney, liver, stomach and colon [16]. During development, transcript variant 1 of *ATP13A3* showed a similar pattern of expression as total *ATP13A3*, with transcript levels highest during E7 and E11. However, the ratio of transcript variant 1 expression to total *ATP13A3* expression increased during development, suggesting that as development progressed from organogenesis to neurogenesis, a larger proportion of the *ATP13A3* present was transcript variant 1 rather than variant 2. The expression profile of variant 1 to total *ATP13A3* was also assessed in the adult mouse brain. Both transcripts showed an identical pattern of expression, with significantly high expression in all brain regions tested and a higher expression within the frontal cortex compared to the total cerebral cortex. Furthermore, the ratio of transcript variant 1 to total *ATP13A3* expression in the brain does not differ significantly between the cerebral cortex, frontal cortex, and brainstem, and this ratio is only slightly lower in the hippocampus and cerebellum. The consistently higher ratio of transcript variant 1 to variant 2 throughout development implies that variant 1 may play a more predominant role. In accordance with the present results, the tissue specificity of the two isoforms was also demonstrated by Schultheis *et al.*, who showed that isoform 1 is predominant in the brain, heart and lung, while isoform 2 is predominant in other tissues including the kidney, small intestine and testis [16].

ATP13A4 has been implicated in language delay and ASD in our previous studies [8, 15]. We determined that *ATP13A4* expression increases in the course of development, with very low levels of expression at E7 and E11 and a marked increase in expression between E11 and E15 [8]. *ATP13A4* expression peaks at E17 and remains quite high in the adult brain, suggesting that it may play an important role during neurogenesis and in the mature nervous system in mice. In the current study, we have shown that *ATP13A4* mRNA expression varied throughout the adult mouse brain and was most highly expressed in cerebellum and brainstem followed by hippocampus and frontal cortex. We also confirmed that the ATP13A4 protein was localized to cells of the cerebellum, brain stem,

hippocampus (particularly dentate gyrus and CA1), frontal and motor cortex, and substantia nigra. The cerebral cortex showed the lowest expression of *ATP13A4* and, as with all of the other P₅ ATPase genes studied, the expression in the frontal cortex was higher than that of the total cerebral cortex. Interestingly, individuals with autism display enlargement or hyperplasia of the cerebral cortex which is greatest in the anterior regions of the cortex (frontal and temporal), and cortical volume increases more slowly from 2 to 9 years of age compared with control individuals [34, 35]. Both hyper- and hypoplasia of the cerebellum and hypoplasia of the brainstem have also been observed in individuals with autism [36, 37]. However, further *in vivo* studies are required to determine whether *ATP13A4* is involved in the development of these brain structures and whether its defects contribute to the pathology of disorders such as autism.

ATP13A5 expression during mouse development showed a distinct trend. This gene was the only one of the four studied which had a higher expression in the adult than at every developmental stage, with relatively low levels in the developing embryo. This would suggest that *ATP13A5* may play a more important role in adult brain function than in its early development. Within the adult brain, *ATP13A5* expression was relatively constant in the frontal cortex, cerebellum, brainstem and hippocampus, and was lowest in the cerebral cortex. This constant level of expression may suggest that *ATP13A5* serves an important role in many regions of the adult brain. It has been shown previously that *ATP13A5* is expressed only within the brain and stomach in the adult mouse, compared to *ATP13A1*, *ATP13A2* and *ATP13A3*, which are expressed in multiple tissues in the mouse, which supports this idea of an important role of *ATP13A5* within the brain [16]. Though *ATP13A4* and *ATP13A5* are most closely related phylogenetically [2, 14-16], they show very different spatial expression profiles within the adult brain. *ATP13A4* expression levels vary widely in the different brain regions tested but *ATP13A5* expression levels are for the most part constant. It is possible that *ATP13A4* and *ATP13A5* perform similar functions due to sequence homologies in the core domains and probable substrate binding sites of the ATPase, although they localized in different brain regions.

Taken together, these results show that P₅ ATPases are expressed at different levels during various developmental stages in the mouse and within tested regions of the adult mouse brain. *ATP13A1*, *ATP13A2* and *ATP13A4* were expressed to the highest degree during neurogenesis, *ATP13A3* on the whole was expressed primarily before the onset of neurogenesis, and *ATP13A5* was expressed to the largest extent in the adult mouse brain. This localization may be representative of their biological function within the nervous system. Due to the observed early or late expression pattern of P₅ ATPases in development, mutations within these genes or defective expression may lead to various pathologies. Although further studies need to determine the cellular and molecular function of P₅ ATPases in the nervous system, this study adds further

evidence for the potential important role of P₅ ATPases during mouse development.

Acknowledgments. This study was supported by the Natural Sciences and Engineering Research Council of Canada (NSERC).

REFERENCES

1. Lutsenko, S. and Kaplan, J.H. Organization of P-type ATPases: significance of structural diversity. **Biochemistry (N.Y.)** 48 (1995) 15607-15613.
2. Axelsen, K.B. and Palmgren, M.G. Evolution of substrate specificities in the P-type ATPase superfamily. **J. Mol. Evol.** 1 (1998) 84-101.
3. Kuhlbrandt, W. Biology, structure and mechanism of P-type ATPases. **Nat. Rev. Mol. Cell Biol.** 4 (2004) 282-295.
4. Paulusma, C.C. and Oude Elferink, R.P. The type 4 subfamily of P-type ATPases, putative aminophospholipid translocases with a role in human disease. **Biochim. Biophys. Acta** 1-2 (2005) 11-24.
5. Folmer, D.E., Elferink, R.P. and Paulusma, C.C. P4 ATPases - lipid flippases and their role in disease. **Biochim. Biophys. Acta** 7 (2009) 628-635.
6. Cronin, S.R., Khoury, A., Ferry, D.K. and Hampton, R.Y. Regulation of HMG-CoA reductase degradation requires the P-type ATPase Cod1p/Spf1p. **J. Cell Biol.** 5 (2000) 915-924.
7. Cronin, S.R., Rao, R. and Hampton, R.Y. Cod1p/Spf1p is a P-type ATPase involved in ER function and Ca²⁺ homeostasis. **J. Cell Biol.** 6 (2002) 1017-1028.
8. Vallipuram, J., Grenville, J. and Crawford, D.A. The E646D-ATP13A4 mutation associated with autism reveals a defect in calcium regulation. **Cell. Mol. Neurobiol.** 30 (2010) 233-246.
9. Suzuki, C. and Shimma, Y.I. P-type ATPase spf1 mutants show a novel resistance mechanism for the killer toxin SMKT. **Mol. Microbiol.** 4 (1999) 813-823.
10. Vashist, S., Frank, C.G., Jakob, C.A. and Ng, D.T. Two distinctly localized p-type ATPases collaborate to maintain organelle homeostasis required for glycoprotein processing and quality control. **Mol. Biol. Cell** 11 (2002) 3955-3966.
11. Jakobsen, M.K., Poulsen, L.R., Schulz, A., Fleurat-Lessard, P., Moller, A., Husted, S., Schiott, M., Amtmann, A. and Palmgren, M.G. Pollen development and fertilization in Arabidopsis is dependent on the *MALE GAMETOGENESIS IMPAIRED ANTHERS* gene encoding a type V P-type ATPase. **Genes Dev.** 22 (2005) 2757-2769.
12. Suzuki, C. Immunochemical and mutational analyses of P-type ATPase Spf1p involved in the yeast secretory pathway. **Biosci. Biotechnol. Biochem.** 11 (2001) 2405-2411.
13. Rand, J.D. and Grant, C.M. The thioredoxin system protects ribosomes against stress-induced aggregation. **Mol. Biol. Cell** 1 (2006) 387-401.

14. Moller, A.B., Asp, T., Holm, P.B. and Palmgren, M.G. Phylogenetic analysis of P5 P-type ATPases, a eukaryotic lineage of secretory pathway pumps. **Mol. Phylogenet. Evol.** 2 (2008) 619-634.
15. Kwasnicka-Crawford, D.A., Carson, A.R., Roberts, W., Summers, A.M., Rehnstrom, K., Jarvela, I. and Scherer, S.W. Characterization of a novel cation transporter ATPase gene (ATP13A4) interrupted by 3q25-q29 inversion in an individual with language delay. **Genomics** 2 (2005) 182-194.
16. Schultheis, P.J., Hagen, T.T., O'Toole, K.K., Tachibana, A., Burke, C.R., McGill, D.L., Okunade, G.W. and Shull, G.E. Characterization of the P5 subfamily of P-type transport ATPases in mice. **Biochem. Biophys. Res. Commun.** 3 (2004) 731-738.
17. Ramirez, A., Heimbach, A., Grundemann, J., Stiller, B., Hampshire, D., Cid, L.P., Goebel, I., Mubaidin, A.F., Wriekat, A.L., Roeper, J., Al-Din, A., Hillmer, A.M., Karsak, M., Liss, B., Woods, C.G., Behrens, M.I. and Kubisch, C. Hereditary parkinsonism with dementia is caused by mutations in ATP13A2, encoding a lysosomal type 5 P-type ATPase. **Nat. Genet.** 10 (2006) 1184-1191.
18. Di Fonzo, A., Chien, H.F., Socal, M., Giraud, S., Tassorelli, C., Iliceto, G., Fabbrini, G., Marconi, R., Fincati, E., Abbruzzese, G., Marini, P., Squitieri, F., Horstink, M.W., Montagna, P., Libera, A.D., Stocchi, F., Goldwurm, S., Ferreira, J.J., Meco, G., Martignoni, E., Lopiano, L., Jardim, L.B., Oostra, B.A., Barbosa, E.R. and Bonifati, V. ATP13A2 missense mutations in juvenile parkinsonism and young onset Parkinson disease. **Neurology** 19 (2007) 1557-1562.
19. Lin, C.H., Tan, E.K., Chen, M.L., Tan, L.C., Lim, H.Q., Chen, G.S. and Wu, R.M. Novel ATP13A2 variant associated with Parkinson disease in Taiwan and Singapore. **Neurology** 21 (2008) 1727-1732.
20. Rakovic, A., Stiller, B., Djarmati, A., Flaquer, A., Freudenberg, J., Toliat, M.R., Linnebank, M., Kostic, V., Lohmann, K., Paus, S., Nurnberg, P., Kubisch, C., Klein, C., Wullner, U. and Ramirez, A. Genetic association study of the P-type ATPase ATP13A2 in late-onset Parkinson's disease. **Mov. Disord.** 3 (2009) 429-433.
21. Santos, A.R. and Duarte, C.B. Validation of internal control genes for expression studies: effects of the neurotrophin BDNF on hippocampal neurons. **J. Neurosci. Res.** 16 (2008) 3684-3692.
22. de Kok, J.B., Roelofs, R.W., Giesendorf, B.A., Pennings, J.L., Waas, E.T., Feuth, T., Swinkels, D.W. and Span, P.N. Normalization of gene expression measurements in tumor tissues: comparison of 13 endogenous control genes. **Lab. Invest.** 1 (2005) 154-159.
23. Thal, S.C., Wyschkon, S., Pieter, D., Engelhard, K. and Werner, C. Selection of endogenous control genes for normalization of gene expression analysis after experimental brain trauma in mice. **J. Neurotrauma** 7 (2008) 785-794.

24. Mwacharo, J., Dunachie, S.J., Kai, O., Hill, A.V., Bejon, P. and Fletcher, H.A. Quantitative PCR evaluation of cellular immune responses in Kenyan children vaccinated with a candidate malaria vaccine. **PloS One** 12 (2009) e8434.
25. Xing, W., Deng, M., Zhang, J., Huang, H., Dirsch, O. and Dahmen, U. Quantitative evaluation and selection of reference genes in a rat model of extended liver resection. **J. Biomol. Tech.** 2 (2009) 109-115.
26. Boda, E., Pini, A., Hoxha, E., Parolisi, R. and Tempia, F. Selection of reference genes for quantitative real-time RT-PCR studies in mouse brain. **J. Mol. Neurosci.** 3 (2009) 238-253.
27. Vandesompele, J., De Preter, K., Pattyn, F., Poppe, B., Van Roy, N., De Paepe, A. and Speleman, F. Accurate normalization of real-time quantitative RT-PCR data by geometric averaging of multiple internal control genes. **Genome Biol.** 3 (2002) RESEARCH0034.
28. Daston, G., Faustman, E., Ginsberg, G., Fenner-Crisp, P., Olin, S., Sonawane, B., Bruckner, J., Breslin, W. and McLaughlin, T.J. A framework for assessing risks to children from exposure to environmental agents. **Environ. Health Perspect.** 2 (2004) 238-256.
29. Rodier, P.M. Chronology of neuron development: animal studies and their clinical implications. **Dev. Med. Child Neurol.** 4 (1980) 525-545.
30. Angevine, J.B., Jr. Time of neuron origin in the diencephalon of the mouse. An autoradiographic study. **J. Comp. Neurol.** 2 (1970) 129-187.
31. Gerfen, C.R., Baimbridge, K.G. and Thibault, J. The neostriatal mosaic: III. Biochemical and developmental dissociation of patch-matrix mesostriatal systems. **J. Neurosci.** 12 (1987) 3935-3944.
32. Bayer, S.A., Wills, K.V., Triarhou, L.C. and Ghetti, B. Time of neuron origin and gradients of neurogenesis in midbrain dopaminergic neurons in the mouse. **Exp. Brain Res.** 2 (1995) 191-199.
33. Kawano, H., Ohyama, K., Kawamura, K. and Nagatsu, I. Migration of dopaminergic neurons in the embryonic mesencephalon of mice. **Brain Res. Dev. Brain Res.** 1-2 (1995) 101-113.
34. Carper, R.A., Moses, P., Tigue, Z.D. and Courchesne, E. Cerebral lobes in autism: early hyperplasia and abnormal age effects. **Neuroimage** 4 (2002) 1038-1051.
35. Carper, R.A. and Courchesne, E. Localized enlargement of the frontal cortex in early autism. **Biol. Psychiatry** 2 (2005) 126-133.
36. Courchesne, E., Saitoh, O., Yeung-Courchesne, R., Press, G.A., Lincoln, A.J., Haas, R.H. and Schreibman, L. Abnormality of cerebellar vermal lobules VI and VII in patients with infantile autism: identification of hypoplastic and hyperplastic subgroups with MR imaging. **AJR Am. J. Roentgenol.** 1 (1994) 123-130.
37. Hashimoto, T., Tayama, M., Murakawa, K., Yoshimoto, T., Miyazaki, M., Harada, M. and Kuroda, Y. Development of the brainstem and cerebellum in autistic patients. **J. Autism Dev. Disord.** 1 (1995) 1-18.